Inorganica Chimica Acta, 16 (1976) 17–28

Photoaction in the Course of Chelate Formation. I. Ligand Photoactivity in the Boric Acid–Benzoylacetone 1/1 Interaction

M. MARCANTONATOS
Department of Inorganic and Analytical Chemistry, University of Geneva, Geneva, Switzerland
Received March 26, 1975

The formation of the 1/1 borobenzoylacetonide chelate in conc. sulfuric acid–ether (8% V/V) solvent is investigated kinetically upon continuous irradiation of 310 nm, corresponding to an intramolecular charge transfer band of the ligand. It can be shown that excitation converts benzoylacetone into a reactive form which contributes to complex formation via excited-state paths, taking place parallel to thermal steps. Probable structures, states and processes of photo-excited species of the ligand are discussed. There are indications that the reactive excited-state form of benzoylacetone is a T_1 disrupted intramolecular hydrogen bonded structure. A combined thermal and photo-excited reaction mechanism is proposed.

Introduction

Most of the research carried out in the highly stimulating field of photochemistry of coordination compounds deals with light-induced reactivity of complexes in condensed phases and photosensitivity of several compounds in the presence of metal ions[1,2].

With the exception of some $Cr(H_2O)_6^{3+}$ photoanation reactions[3] and the Fe^{2+}–thionine photointeractions[1a], systematic investigations on the effect of irradiating the ligand or the central group during complex formation have not, to our knowledge, as yet been reported. It appears also that such investigations on chelate formation have not been, up to now, carried out.

The present work is the first part of a research carried out on these lines and actually under way. It presents an analysis and includes discussion of results obtained from investigations on the rate of formation of the 1/1 borobenzoylacetonide chelate in conc. H_2SO_4–ether solvent, upon uninterrupted irradiation of 310 nm corresponding to the ICT band[4,5] of benzoylacetone. Preliminary investigations on the rate of chelate formation showed that increasing light intensity causes a regular lowering in the overall forward rate constant and a decrease in the reverse one. Since no detectable photodecomposition of benzoylacetone or chelate has been found with the intensities used in these experiments, excited-state ligand reactivity and contribution to complex formation were, therefore, considered for investigation.

Experimental

Reagents and Solutions

Benzoylacetone (Fluka) was purified by double recrystallisation with water (tridistilled)/ethanol (G.R. Merck), 15% V/V. Boric and sulfuric acids were G. R. Merck. The latter (H_2SO_4, d = 1.84) was regularly checked conductometrically[6,7] and, if necessary, the percentage adjusted to 96%. Ether (0.02% water max. content) was G. R. Merck.

In order to minimize ether solvolysis ($EtOEt + 3H_2SO_4 \xrightarrow{T} 2EtHSO_4 + H_3O^+ + HSO_4^-$)[8], the "sulfuric (96%) acid/EtOEt, (8% V/V)" solvent (SE) was prepared by pouring overcooled viscous EtOEt portions on frozen H_2SO_4, and then allowing the mixture to reach room temperature. Solutions of benzoylacetone were always prepared, before each experiment, by dissolving the compound in SE solvent, while boric acid solutions in SE were made before each experiment from a $10^{-1}M$ BO_3H_3 stock sulfuric acid solution and SE solvent under the same conditions as described above for the preparation of the SE solvent. As checked by the HMCB fluorometric method[9], BO_3H_3 sulfuric solutions, stocked in quartz flasks, were perfectly stable over several months.

Apparatus

Irradiations of 3 ml non-deaerated SE solutions of BO_3H_3 + benzoylacetone contained in a 1 cm-depth, well-tight, quartz cell were carried out at 20 ± 1 °C in a Perkin–Elmer MPF-2A spectrofluorometer assembly, by setting the excitation monochromator at 310 nm and varying its slit width. Incident light intensities $I_o' = SI_o(Nh\nu/min)$ were measured, under exactly the same conditions, by a ferric oxalate actinometer[10]. For a given excitation slit, intensities thus obtained from a

set of parallel measurements were reproducible to ± 2%. Eventual variations from one experiment to another were corrected from a I_o' *vs.* slit width graph.

Kinetics of the borobenzoylacetonide chelate formation was monitored simultaneously with irradiation by setting the emission monochromator at 382 nm and following the fluorescence of the chelate (max. emission at 382 nm with excitation at 341 nm). In all cases, with conditions $[A]_o/[R]_o = 80$ to 400 (where $[A]_o$ and $[R]_o$ stand for initial concentrations of boric acid and benzoylacetone) the kinetics of forward pseudo-first-order reversible formation of the chelate were observed.

Observed rate constants for:

$$A + R \underset{\overleftarrow{k}}{\overset{\vec{k}}{\rightleftharpoons}} AR \qquad (1)$$

were extracted from the linear plots $\ln(F_e/F_e-F) = k_{obs}t = (\vec{k}[A]_o + \overleftarrow{k})t$ (where F_e and F are fluorescence intensities at equilibrium and time t) and expressed as a function of $[A]_o$ to get, for a given irradiation intensity, valucs of $\vec{k}$ and $\overleftarrow{k}$ (sce figure 2).

Regression coefficients for linear $\ln(F_e(F_e-F)$ *vs.* t plots were seldom inferior and most often superior to 0.999.

For our experimental conditions, the average intensity $I_{a(i)}(Nh\nu/t \times min)$, absorbed by a given species i, is expressed by:

$$I_{a(i)} = I_o'V^{-1}G\varepsilon_i C_i \qquad (2)$$

where

$$G = (1-\exp[-2.3031\Sigma_i\varepsilon_i C_i])/\Sigma_i\varepsilon_i C_i \simeq \text{constant}$$

In fact, in the course of the borobenzoylacetonide chelate (AR) formation, the main absorbing species at 310 nm are the benzoylacetone (BZA) conjugate chelate form (R), its protonated one RH (see later) and the chelate.

Now, assuming steady-state conditions for RH (see under Reaction Mechanism), $[RH] = \gamma[R]_o$, and taking $\varepsilon_{RH} = q\varepsilon_R$:

$$G = \frac{1-e^{-2.3031([1+(q-1)\gamma]\varepsilon_R[R]_o + (\varepsilon_{AR}-\varepsilon_R)[AR])}}{[1+(q-1)\gamma]\varepsilon_R[R]_o + (\varepsilon_{AR}-\varepsilon_R)[AR]}, \qquad (3)$$

we get:

$G \simeq 2.3031 - 2.652([1+(q-1)\gamma]\varepsilon_R[R]_o + (\varepsilon_{AR}-\varepsilon_R)[AR])^2 - \cdots$ which becomes a constant if $(\varepsilon_{AR}-\varepsilon_R)[AR] \ll [1+(q-1)\gamma]\varepsilon_R[R]_o$.

From $\varepsilon_R^{310} = 15200$ (BZA spectrum in EtOEt), $\varepsilon_{AR}^{310} = 13800$ (BZA + BO_3H_3 spectrum in SE, with BO_3H_3 calculated for complete complexation of BZA) and from (see (1)):

$$[AR] = [R]_o\left(1 - \frac{\overleftarrow{k}}{\vec{k}[A]_o + \overleftarrow{k}} - \frac{\vec{k}[A]_o}{\vec{k}[A]_o + \overleftarrow{k}}\exp[-(\vec{k}[A]_o + \overleftarrow{k})t]\right), \qquad (4)$$

calculated values of G (Table I), using (3) and taking q = 1, show that G is a constant within ± 1% for all kinetic runs with $1.33 \times 10^{-5} \leq I_o' \leq 4.48 \times 10^{-5}$.

Results and Discussion

Preliminary Considerations

From Figures 1(a) to (g), it can be seen that there is no noticeable difference in the electronic absorption and emission spectra, as well as T_1–S_o radiative lifetimes of benzoylacetone and its 1/1 boron chelate, compared to those taken after 60 min irradiation (longest time for the attainment of chelate formation equilibrium) of 4.48×10^{-5} Nhν/min intensity, which was the highest one used.

Also, with increasing intensity, no significant variation in the complex equilibrium concentrations (Table II) occurred, and in all cases the kinetics of complex formation verified, without deviation, the overall reaction:

$$B + R \underset{\overleftarrow{k}}{\overset{\vec{k}}{\rightleftharpoons}} BR \qquad (5)$$

B, R and BR standing for boron species, ligand and complex.

However, the analysis of the kinetics upon continuous ligand excitation reveals two interesting effects: a linear increase of the reverse rate constant $\overleftarrow{k}$ with light intensity and a decrease of $\vec{k}$ (Figure 2 and 3, table III).

TABLE I. G Values for Different Reaction Times ($[R]_o = 10^{-5}$).[a]

$I_o' \times 10^5$ (Nhν/min)	$A_o \times 10^3$ (*M*)	G(cm)		
		t = 1 min	t = 10 min	t = ∞
1.33	1.4	1.944	1.949	1.954
	4.	1.945	1.956	1.962
4.48	0.8	1.943	1.945	1.948
	4.0	1.945	1.954	1.958

[a] G(t = 0) = 1.944.

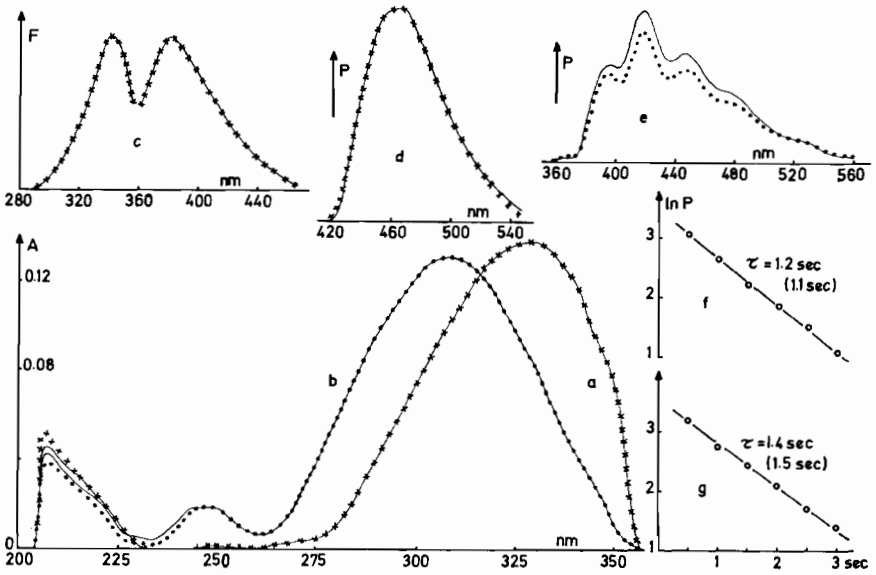

Figure 1. Spectral features of irradiated (—) (310 nm) and non-irradiated solutions of benzoylacetone (...) and of its 1/1 boron chelate (xxx) in SE solvent and semilogarithmic phosphorescence dacay plots. (a) Absorption (8.5×10^{-6} BZA + 2×10^{-3} BO_3H_3); (b) absorption (8.5×10^{-6} BZA); (c) excitation-fluorescence; (d) phosphorescence; (g) mean lifetime of the chelate (8.5×10^{-6} BZA + 2×10^{-3} BO_3H_3); in parentheses, value given in the lit.[14]; (e) phosphorescence; (f) mean lifetime of BZA (5×10^{-3}).

TABLE II. Equilibrium Chelate Concentrations ($\times 10^6$ M^{-1})[a] for Various Intensities I_o'(Nhν/min)×($[R]_o = 10^{-5} M$).

$[A]_o \times 10^3$ \ $I_o \times 10^5$	1.33	2.04	2.83	4.00	4.48
0.8			3.4	3.1	2.7
1.					
1.4	4.7	4.9		4.4	
2.	5.5	5.4	5.6	5.2	5.1
2.5	6.3	5.8			5.8
3.	6.5	6.4	6.6	6.2	6.1
3.5	6.9	6.6			6.4
4.		7.4	7.3		7.2

[a] Obtained from $F_e/\varphi_1 \cdot l$, where F_e are fluorescence intensities at equilibrium, converted for $I_o' = 1.33 \times 10^{-5}$ Nhν/min, and where φ_1 is the corresponding apparent fluorescence efficiency (obtained from kinetic and equilibrium data of dark complexation).
[b] $[A]_o$ and $[R]_o$: initial concentrations of boric acid and benzoylacetone.

TABLE III. $\vec{k}$ (M^{-1} min^{-1}) and $\overleftarrow{k}$ (min^{-1}) for Various Intensities I_o'(Nhν/min).

$I_o' \times 10^5$	0	1.33	2.04	2.83	4.00	4.48
$\vec{k} \pm s$	22.28 ± 0.8	20.51 ± 0.64	19.45 ± 0.7	18.32 ± 0.45	16.52 ± 0.12	16.15 ± 0.67
$(\overleftarrow{k} \pm s) \times 10^3$ [a]	35 ± 1	47 ± 1	48 ± 2	53 ± 1	60 ± 0.3	61 ± 2

[a] $s = t\sigma/\sqrt{N}$; σ = standard error; t value for a 95% probability.

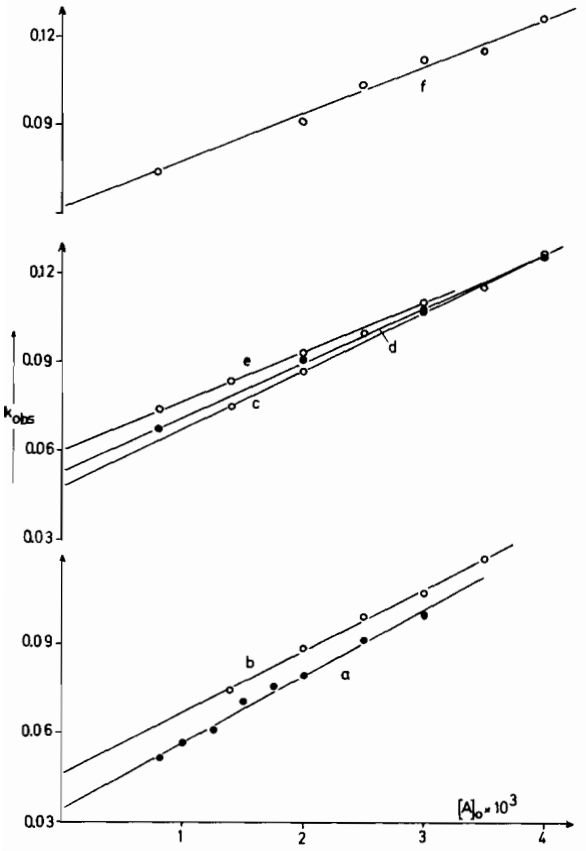

Figure 2. k_{obs} *vs.* initial boric acid concentration $[A]_o$, for various intensities I_o' at 310 nm. I_o' x 10^5 Nhν/min: (b) 1.33, (c) 2.04, (a) 2.83, (e) 4.0, (f) 4.48. (a) values from dark complexation monitored with excitation at 341 nm (excitation band maximum of the chelate).

If there is ligand photoactivity and if excited-state paths are assumed to operate parallel to ground-state steps in the complex formation, the observed variation of k is not so unexpected. In fact, as it can be shown that complex formation takes place thermally through a non-chelate tetrahedral boron intermediate R–B[11], one can consider the simple reaction scheme (6):

$$\begin{array}{ccccc} R^* + B & \xrightarrow{k^*} & (R\text{–}B)^* & & \\ \uparrow h\nu & & \downarrow k' & & \\ R + B & \underset{k_{-1}}{\overset{k_1}{\rightleftharpoons}} & (R\text{–}B) & \underset{k_{-2}}{\overset{k_2}{\rightleftharpoons}} & RB \end{array} \qquad (6)$$

for which the expressions (see also (2)):

$$\frac{d[R^*]}{dt} = I_a - k^*[R^*][B] = \varphi_R \varepsilon_R V^{-1} G I_o'[R] - k^*[R^*][B]_o$$

$$\frac{d[(R\text{–}B)^*]}{dt} = k^*[R^*][B]_o - k'[(R\text{–}B)^*]$$

$$\frac{d[R\text{–}B]}{dt} = k_1[R][B]_o + k_{-2}[RB] + k'[(R\text{–}B)^*] - (k_{-1} + k_{-2})[R\text{–}B],$$

together with the usual steady-state assumptions, give the following rate expression for complex formation:

$$\frac{d[RB]}{dt} = \frac{(k_2 \varphi_R \varepsilon_R V^{-1} G I_o' + k_2 k_1 [B]_o)[R] - k_{-1} k_{-2}[RB]}{k_{-1} + k_2} \qquad (7)$$

Solution of this relation is:

$$\ln \frac{[RB]_e}{[RB]_e - [RB]} = k_{obs} t$$

where

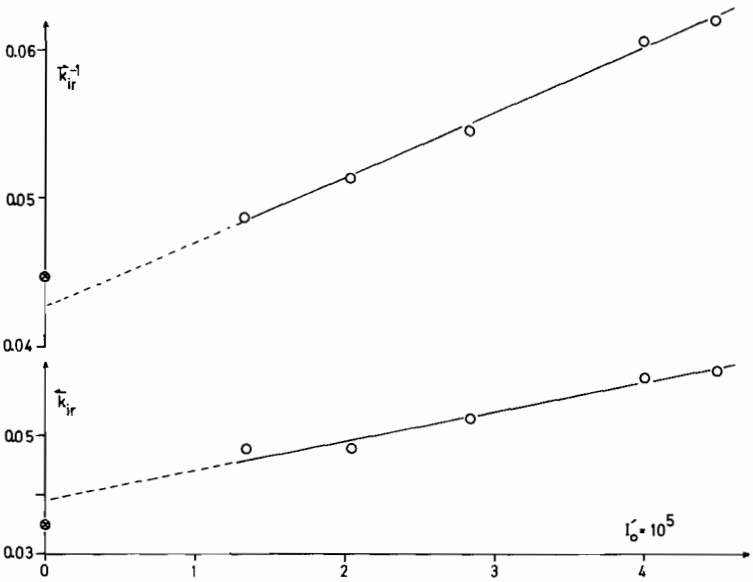

Figure 3. Reverse rate constant $\overleftarrow{k}_{ir}$ and $1/\overrightarrow{k}_{ir}$ (values upon continuous irradiation) as a function of I_o'. ⊕: value for dark complexation.

$$k_{obs} = \frac{k_2 k_1 [B]_o}{k_1 + k_2} + \frac{k_2 \varphi_R \varepsilon_R V^{-1} G I_o' + k_{-1} k_{-2}}{k_{-1} + k_2} = \vec{k}[B]_o + \overleftarrow{k} \quad (8)$$

thus showing a linear dependence of $\vec{k}$ upon irradiation intensity, with the thermal term $k_{-1}k_{-2}/(k_{-1}+k_2)$ as intercept.

However, the combined thermal and photoexcited reaction scheme (6) does not account for the observed decrease of $\vec{k}$.

Possible photosensitivity of the intermediate R–B:

$$R\text{–}B \xrightarrow{h\nu} (R\text{–}B)^* \xrightarrow{k''} \quad (9)$$

cannot explain this lowering, since in this case, whether (R–B) is a lowest singlet or triplet, one obtains:

$$\frac{d[(R\text{–}B)^*]}{dt} = \varphi_{R\text{–}B}\varepsilon_{R\text{–}B}V^{-1}GI_o'[R\text{–}B] + \varphi_R\varepsilon_R V^{-1} G I_o'[R] - (k' + k'')[(R\text{–}B)^*],$$

$$[(R\text{–}B)^*] = \varphi_R\varepsilon_R V^{-1} G I_o'[R]/(k' + k''); \quad ([R\text{–}B] \ll [R]),$$

and

$$\frac{d[R\text{–}B]}{dt} = \frac{k'\varphi_R\varepsilon_R V^{-1} G I_o'[R]}{k' + k''} - \varphi_{R\text{–}B}\varepsilon_{R\text{–}B}V^{-1} G I_o'[R\text{–}B] + k_1[R][B]_0 + k_{-2}[RB] - (k_{-1} + k_2)[R\text{–}B], \quad (10)$$

in which relation $\varphi_{R\text{–}B}\varepsilon_{R\text{–}B}V^{-1}GI_o'[R\text{–}B]$ must be of negligible magnitude compared to the other kinetic terms, thus leading to an expression analogous to (7).

The variation of $\vec{k}$ can, however, be explained by possible photoactivity of benzoylacetone's protonated species, so that its forms in the excited state, as well as those of the non-protonated ligand, have to be considered.

Probable Ligand Ground and Excited-state Forms

It has been shown that benzoylacetone (BZA) conjugate chelate form (R) (see (11)), characterised by an intense ICT band[4] at 305 nm, is in equilibrium and in excess over the diketo form (R_c) in non polar solvents. In the solvent SE used in this work, evidence for the formation of protonated species (RH) in the ground state and indications on probable R and RH forms in the excited state can be obtained from electronic absorption and emission spectra of BZA.

It has been found that, when the solvent is changed from ether (EtOEt) to SE solvent, the electronic absorption spectrum of BZA displays a 4 nm bathochromic shift in the ICT band[11]. For this change in medium, lowerings (from 77 K phosphorescence spectra) in the perturbed vibrational frequencies of C–OH (perturbed by some double bond character in R) and of C=O in the diketo form (R_c) have also been observed.*

These changes in spectral features are partly due to the increase in polarity of the medium, but result mainly from the displacement of BZA towards protonated species:

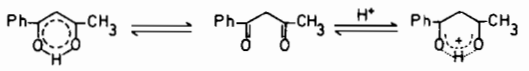

(11)

* $\nu(EtOEt) - \nu(SE) = \Delta\nu$, $\Delta\nu COH \doteq 10$ cm^{-1}, $\Delta\nu CO = 20$ cm^{-1}. In the case of dibenzoylmethane, $\Delta\nu COH = 50$ cm^{-1}, $\Delta\nu CO = 3$ cm^{-1}.

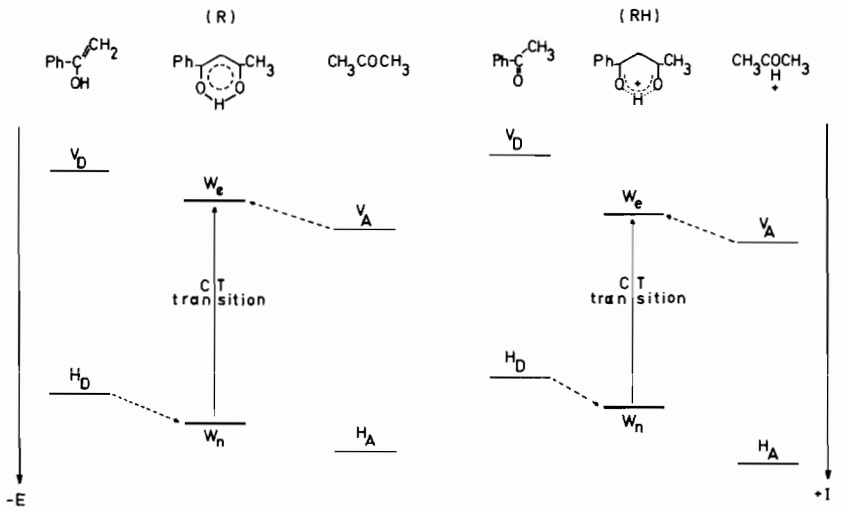

Figure 4. Qualitative representation of CT states of benzoylacetone conjugate chelate and protonated forms. E: energies of the highest occupied (H_D, H_A) and lowest vacant (V_D, V_A) MO's of donors (D) and acceptors (A). I: ionization potential (referring to H_D and H_A).

This can be deduced from an enery level diagram (Figure 4), using the principles of the ICT theory[5]. It can be seen that the interaction of H_D and V_A leads to levels W_n and W_e, whose difference is less for RH than for R, since in the case of RH the energy of the highest occupied MO of the acceptor must be lower (higher I value) than in R and the energy of the donor's highest occupied MO must be higher (lower I value) than in R.

In addition, owing to the strongest lone-pair electron donation to H^+ of the acceptor's oxygen in RH, electron migration ($RH \rightarrow Ph^+=C-CH=C-CH_3$ (X)) from

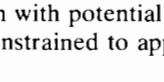

donor to acceptor is more important (largest contribution of the lowest unfilled π^* orbital) than in R and R_c. Bond orders of C–OH and C=O consequently decrease[5a] (compare R with some double bond character in C–OH, and R_c to X), accounting thus for the above mentioned lowering in νCOH and νCO.

Finally, in the case of dibenzoylmethane (DBM), whose absorption[11] and fluorescence spectrum* (Figure 5) exhibits analogous (red) shifts when the medium is changed from EtOEt to EtOEt–H_2SO_4 and then to H_2SO_4, excitation-fluorescence band maxima splitting first increases then diminishes and finally becomes approximatively constant (Figure 6) for H_2SO_4 concentrations where most probably DBM is completely in the monoprotonated form (cryoscopic factor $\nu = 2$ in 100% H_2SO_4)[12].

A hypothetical diagram with potential energy curves W *vs.* r in coordinates constrained to appropriate configurational ones, would show that such variations up to a certain H_2SO_4 concentration are due to the presence of more than one absorbing–emitting species for which, in addition, interconversion may take place in the ground state as well as in the excited state.

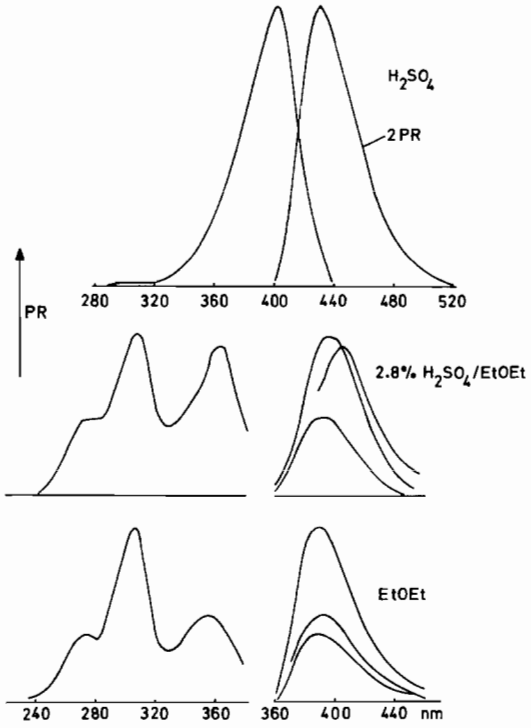

Figure 5. Excitation and fluorescence spectra of dibenzoylmethane for different solvent compositions. PR: photomultiplier response.

* Fluorescence quantum yield of benzoylacetone is too low to make any accurate study of excitation-emission spectral modifications with medium composition.

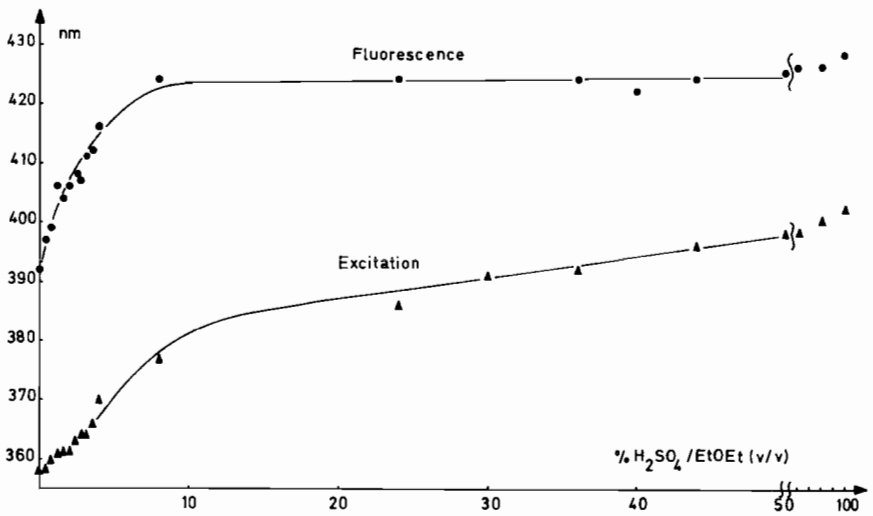

Figure 6. Variation of band maxima wavelength of dibenzoylmethane with solvent composition. [DBM] = $2 \times 10^{-5} M$.

Undoubtedly, beyond a certain concentration of H_2SO_4 in EtOEt, medium effects other than protonation will occur. Nevertheless, lowest singlet excited-state protolysis of the intramolecular hydrogen bond in R, occurring to some extent within the life-time of this state and for somewhat lower proton concentration than in the ground state (Figure 6), is not to be excluded and may also occur in the lowest triplet.

Also, since with 310 nm light insignificant excitation of the diketo forms of DBM and BZA occurs[11] (which, moreover, are in low concentrations in SE solvent) and since basicity of the hydrogen bonded ring in the excited state seems to increase (Figure 6), possible round and excited-state processes and forms (the latter being presented by the largest contributing resonance structures) may be portrayed as follows:

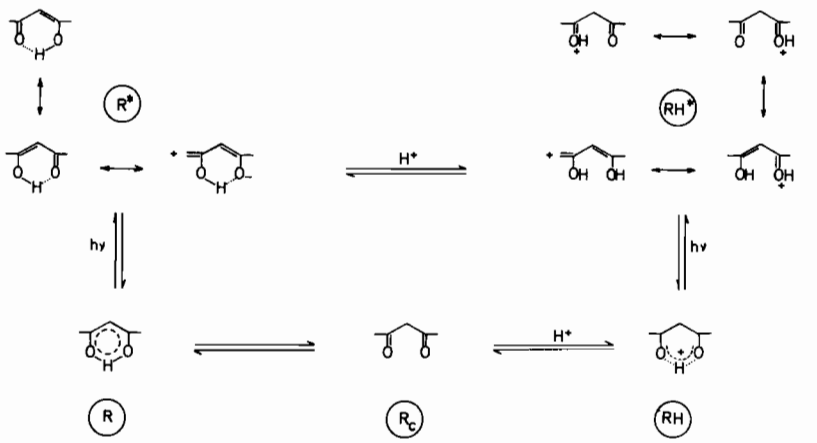

(12)

Proposal of Reaction Mechanism

In view of the preceding considerations, the following combined thermal and photoexcited reaction mechanism (Figure 7) seems to fit with the experimental results:

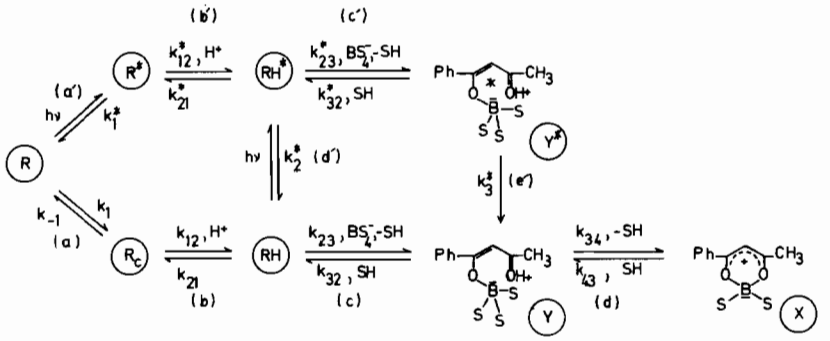

Figure 7. Proposed reaction scheme.

Steps (a) to (d) are the propsed ground-state mechanism[11], while those (a') to (e') represent the photoexcited pathways, with k_1*, k_2* and k_3* absorbing constants for monomolecular radiative or radiationless processes and eventually biomolecular quenching.

SH stands for H_2SO_4 and BS_4^- for the tetra(hydrogensulfato)borate ion, which is assumed to be the only reacting boron species in order to simplify calculations. This, however, does not exclude ligand interaction with possible $B(OH)(HSO_4)_3^-$ species[13], but it can readily be shown that as long as $B(OH)(HSO_4)_3^-$ parallel interaction with ligand leads to the same intermediate (Y), kinetic expressions are of the same form as if a single boron species were to react.

In fact, the form in which boron species might occur in SE solvent can be given by making the following assumptions[11]:

i) Since in 96% H_2SO_4, BO_3H_3 is mainly in the form of BS_4^- (S = $-OSO_3H$) in equilibrium probably with $B(OH)S_3^-$[13], and since free water molecules must be in negligible concentration in SE solvent:

$$HSO_4^- + H_3O^+ \xrightleftharpoons{H_2O} H_2SO_4 \xrightleftharpoons{EtOEt} (Et)_2OH^+ + HSO_4^-,$$

any extensive de-hydrogensulfatation of BS_4^- and $B(OH)S_3^-$ is improbable when BO_3H_3/SE solutions are prepared in an appropriate manner (see Experimental) from BO_3H_3 sulfuric solution and H_2SO_4/EtOEt.

In this case, it can be seen from:

$$\begin{array}{ccc} B(OH)S_3^- & \xrightleftharpoons{K_B,2SH,-H_3O^+,-S} & BS_4^- \\ K_b,H^+_{(Z)} \Big\downarrow & & \Big\uparrow K_{b'},H^+_{(Z)} \\ [B(OH)S_3]H_{(Z)} & & [BS_4]H_{(Z)} \end{array}$$

$K_B' = K_B[SH]^2([H_3O^+][S^-])^{-1} = [BS_4^-]/[B(OH)S_3^-]$,

$J = 1 + K_b[H^+_{(Z)}] + (1 + K_{b'}[H^+_{b'}[H^+_{(Z)}])KB'$,

Total boric acid conc.: $[A] = [B(OH)S_3^-]J = [BS_4^-]JK_B'^{-1}$

$H^+_{(Z)}$: solvated proton,

that, if interactions of r_H(r_H: RH or RH*) with BS_4^- and $B(OH)S_3^-$ lead to y (y: Y or Y*),

$$\frac{d[y]}{dt} = k_{b'}[r_H][BS_4^-] + k_b[r_H][B(OH)S_3^-] \pm \ldots.$$

$$= (k_bK_B' + k_b)J^{-1}[A][r_H] \pm \ldots\ldots = k_{bb'}[A][r_H] \pm \ldots. \quad (13)$$

ii) In the case where de-hydrogensulfatation takes place effectively to some extent (presence of free water traces) and leads to non ionic species $B(OH)_{3-i}S_i$ ($3 \geq i \geq 0$) too, it can be shown[11] that several relations, as long as only anionic boron species are assumed to interact with the ligand RH, lead to a kinetic expression analogous to (13).

According to the proposed reaction scheme (Figure 7), the main link between excited and ground-state complexation is the deactivation [step (e')] of the non-chelate tetrahedral boron intermediate Y*. Its yield or concentration can be derived from rate expressions of R* and RH* formation and Y* disappearance. However, if states of these species are not specified, any description of excited-state kinetic situations may be insufficient. Consequently, a number of considerations concerning the states of BZA's excited forms have to be introduced.

States and processes of ligand photoexcited forms

From the more elaborated scheme (with neglected ground singlet–triplet and triplet–triplet quenchings) for steps (a'), (b'), (c') and (d'):

$$r \xrightarrow{I_a} {}^1r \quad (14)$$

$${}^1r \xrightarrow{k_{ST}} {}^3r \quad (15)$$

$${}^{1,3}r \xrightarrow{k_{F,P}} r \quad (16)$$

$${}^{1,3}r \xrightarrow{k_{C,TS}} r \quad (17)$$

$${}^{1,3}r \xrightarrow{{}^{1,3}k_Q,Q} r \quad (18)$$

$${}^{1,3}RH \underset{{}^{1,3}k_{12},H^+}{\overset{{}^{1,3}k_{21}}{\rightleftharpoons}} {}^{1,3}R \quad (19)$$

$${}^{1,3}RH \underset{{}^{1,3}k_{32},SH}{\overset{{}^{1,3}k_{23},BS_4^-}{\rightleftharpoons}} {}^{1,3}Y \quad (20)$$

(where r = R or RH; 1,3 = excited singlet or triplet; F,P = fluorescence or phosphorescence; ST = $S_1 \rightarrow T$ crossing; C,TS = internal conversion or $T_1 \rightarrow S$ crossing; Q = mainly oxygen as quencher), it can be readily deduced that interaction of BS_4^- with RH in a given excited state is possible only if lifetimes of monomolecular or pseudo-monomolecular processes in (19) and (20) are of comparable magnitude to:

$${}^1\tau_R = 1/(k_F + k_C + k_{ST} + {}^1k_Q[Q]) \quad (21)$$

or

$${}^3\tau_R = 1/(k_P + k_{TS} + {}^3k_Q[Q]) \quad (22)$$

Excited state reversible protolysis of R seems feasible in the T_1 state and, as has been shown previously, this is quite possible in S_1. On the contrary, for interactions of the (20) type, this appears to be highly improbable in the S_1 but still possible in the T_1 state.

In fact, in view of the very low fluorescence of R in EtOEt or SE solvent at room temperature, a $\sim 1\%$ fluorescence yield can be roughly attributed to R, so that for $\varepsilon_{max\,(R)} = 15200$, the approximation $\tau^o \sim 10^{-4}/\varepsilon_{max}$, together with (21) and $k_{F\,(R)} = 1/\tau^o{}_{F\,(R)}$ gives as order of magnitude ${}^1\tau_R \sim 10^{-10}$ sec.

On the other hand, from 77K total and phosphorescence emission in EtOEt, $(\Phi_{P\,(R)}/\Phi_{F\,(R)})_{77} \simeq 2.3$ and taking $(\Phi_{F\,(R)})_{77}/\Phi_{F\,(R)} \sim 10$ (approximate evaluation), it follows that for 77K:

$$\Phi_{P\,(R)} = k_P{}^3\tau\Phi_{ST} \sim 0.23$$

Assuming that, for these conditions, $k_C + {}^1k_Q[Q] \ll k_F + k_{ST}$ and as $\tau^o{}_{P\,(R)} = 1.1$ sec[14]:

$${}^3\tau_R = \Phi_{P\,(R)}\tau^o{}_{P\,(R)}/(1-\Phi_{F\,(R)}) \sim 0.28 \text{ sec}$$

which, even as an order of magnitude, is undoubtedly guite large for room temperature solutions (present work conditions). But the more probable value ${}^3\tau_R \sim 10^{-3}$ sec for a fluid medium still shows that it is by far more favourable than ${}^1\tau_R$ for interactions of type (19) and (20) to occur.

Unfortunately it is impossible, from the body of data accumulated in this work, to determine rate constants of the (19) and especially (20) precesses and to compare them with the ${}^{1,3}\tau_R$ thus evaluated. It is, nevertheless, possible to make the following rough estimations.

From the values of the overall forward and reverse rate constants $\vec{k}$, $\overleftarrow{k}$ for dark complexation, expressed according to Figure 7 by:

$\vec{k} = k_{34}k_{23}K_1K_{12}[H^+]/k'_{32} + k_{34} = 0.37M^{-1}sec^{-1}$,
(where $K_1 = k_1k_{-1}^{-1}$ and $K_{12} = k_{12}k_{21}^{-1}$)

$\overleftarrow{k} = k_{32}'k_{43}'/k_{32}' + k_{34} = 5.8 \times 10^{-4}sec^{-1}$,

it can be seen that $k_{32}' > \overleftarrow{k}$ and $k_{23} > \vec{k}$.

Indeed, from $k_{32}' = \overleftarrow{k}a/(1-b)$, where $a = k_{34}/k_{43}'$ and $b = \overleftarrow{k}/k_{43}'$, a must be greater than unity because of the well-known boron tetrahedral chelate stabilisation, and $b < 1$. Also, in the expression $k_{23} = \vec{k}(1+C)d$, where $c = k_{34}/k_{32}'$ and $d = k_{32}'/K_2K_{12}[H^+]$, c is probably less than unity because ring closure involves expulsion of firmly bound H^+ and $-OSO_3H$, and d may be much larger than unity, since $K_1 < 1$, because of the strong tendency of BA to transform into the conjugate chelate structure.

If then, for dark complexation, upper limits are taken as $k_{23} \sim 37M^{-1}$ sec^{-1} and $k_{32}' \sim 0.06$ sec^{-1}, forward step in (20) seems possible, since RH lowest triplet configuration may be by far more favorable for BS_4^- approach and interaction than its S_o configuration. The reverse step in (20) remains, however, questionable but not strictly excluded, since a much more distorted configuration of Y in its lowest triplet is to be expected.

On the basis of these considerations and according to the extended (14) to (20) scheme, rate expressions for R* and RH* are:

$$\frac{d[^3R]}{dt} = \Phi_{ST}[(^1k + {}^1k_{12}[H^+] - {}^1k_{21}[^1RH][^1R]^{-1})[^1R]]$$
$$-(^3k + {}^3k_{12}[H^+] - k_{21}[^3RH][^3R]^{-1})[^3R] \quad (23)$$

where

$$\Phi_{ST} = k_{ST}/(^1k + {}^1k_{12}[H^+] - {}^1k_{21}[^1RH][^1R]^{-1}) \quad (24)$$

$$^1k = k_F + k_C + {}^1k_Q[Q] + k_{ST} \quad (25)$$

$$I_a = (^1k + {}^1k_{12}[H^+] - {}^1k_{21}[^1RH][^1R]^{-1})[^1R] \quad (26)$$

$$^3k = k_P + {}^3k_Q[Q] + k_{TS}, \quad (27)$$

and

$$\frac{d[^3RH]}{dt} = \Phi_{ST}'[(^1k' + {}^1k_{21} - {}^1k_{12}[H^+][^1R]$$
$$[^1RH]^{-1})[^1RH]] - (^3k' + {}^3k_{21} + {}^3k_{23}[BS_4^-] -$$
$${}^3k_{12}[H^+][^3R][^3RH]^{-1} - {}^3k_{32}'[^3Y][^3RH]^{-1})[^3RH], \quad (28)$$

where

$$\Phi_{ST}' = k_{ST}'/(^1k' + {}^1k_{21} - {}^1k_{12}[H^+][^1R][^1RH]^{-1}) \quad (29)$$

$$^1k' = k_F' + k_C' + {}^1k_Q'[Q] + k_{ST}' \quad (30)$$

$$^3k' = k_P' + {}^3k_Q'[Q] + k_{TS}' \quad (31)$$

Assuming steady-state conditions for ^3R, ^3RH and ^3Y, then from (23), (28) and:

$$\frac{d[^3Y]}{dt} = {}^3k_{23}[BS_4^-][^3RH] - (^3k_{32}' + k_3^*)[^3Y], \quad (32)$$

where $^3k_{32}' = {}^3k_{32}[SH]$,

one obtains:

$$[^3Y] = k_3^{*-1}[(\Phi_{ST} - \Phi_{ST}')^1k_{12}[H^+][^1R] +$$
$$[\Phi_{ST}'(^1k_{21} + {}^1k') - \Phi_{ST}{}^1k_{21}][^1RH] + \Phi_{ST}{}^1k$$
$$[^1R] - (^3k[^3R] + {}^3k'[^3RH])], \quad (33)$$

but the relative magnitudes of yields of intersystem-crossing Φ_{ST} and Φ_{ST}' have to be considered now.

As shown in Figure 8, the 77 K phosphorescence emission of BZA in clear EtOEt glasses (Figure 8a' and 8a'') decreases on protonation (Figure 8b' and 8b''), the effect being larger on the emission of the diketo form (predominantly excited at 255 nm[14]) than that of the conjugate chelate (excited at 362 nm[14]). If it is assumed that this decrease is due to a much lower phosphorescence yield of the protonated form ($\Phi_{P(RH)} \ll \Phi_{P(R)}$ or $\Phi_{P(Rc)}$), the peculiar variation of BZA emission on changing from EtOEt to clear SE glasses is not unexpected. As a matter of fact, in 77 K and EtOEt solid matrix, there is a definite proportion of R_c and R forms. On forming RH by protonation, equilibria at 77 K are displaced towards the intermolecular hydrogen bonded structure, but as the intramolecular H-bonded one is greatly stabilised, the main effect is on the diketonic form.

However, it is not evident that the observed phosphorescence decrease reflects a $\Phi_{ST(RH)} \ll \Phi_{ST(R)}$ or $\Phi_{ST(R_c)}$ situation. $k_{DP}(= k_{TS} + {}^3k_Q[Q])$ cannot necessarily be neglected as is done inconclusively in many cases, and therefore $k_{TS(RH)} \gg k_{TS(R)}$ or $k_{TS(R_c)}$ may also be responsible for such a phosphorescence intensity diminution.

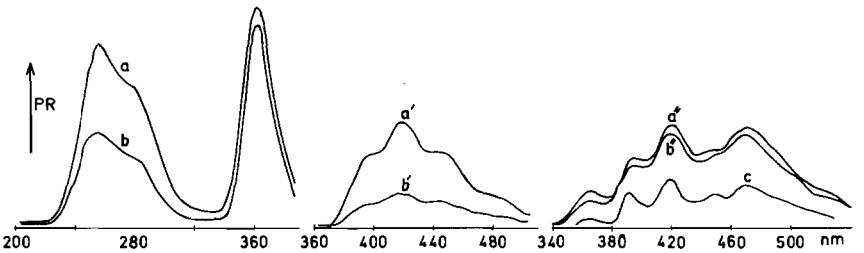

Figure 8. Excitation and phosphorescence spectra of BZA ($5 \times 10^{-3}M$)) in EtOEt and SE glasses. PR: photomultiplier response. a, a', a'': EtOEt; a': excitation at 255 nm; a'': excitation at 362 nm; a' and a'': higher resolution; b, b', b'', c: SE solvent; b', b'', c: higher resolution.

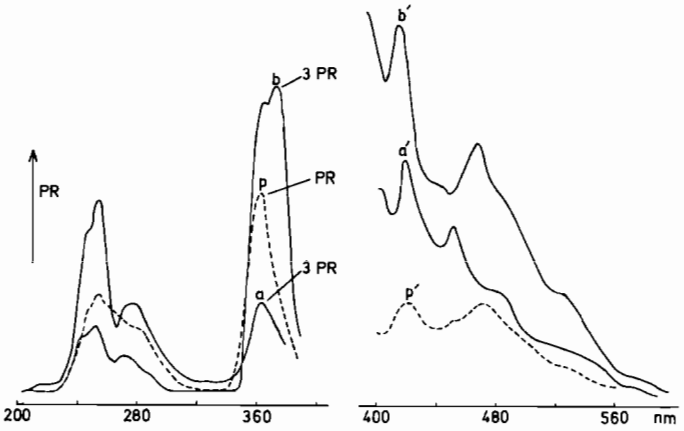

Figure 9. Total excitation and emission spectra of BZA ($5 \times 10^{-3} M$) in EtOEt and SE glasses. PR: photomultiplier response; a and a′: EtOEt (a′ excitation at 362 nm); b and b′: SE solvent (b′ excitation at 373 nm); p and p′: excitation (362 nm) and phosphorescence in SE solvent; p′: higher resolution; a′ and b′: higher resolution, but augmented sensitivity.

Nevertheless, Figure 9 unambiguously indicates that $S_{1(RH)} \rightsquigarrow T_{(RH)}$ crossing is by far less efficient than $S_{1(R)} \rightsquigarrow T_{(R)}$, so that the above alternative based on k_{DP} considerations is of no importance.

In fact, the total emission at 77 K and in SE glasses (Figure 9b′) is approximately three times more intense than in EtOEt glasses (Figure 9a′) and its excitation band at 373 nm (Figure 9b) is practically absent in EtOEt, therefore being attributable to the RH form. If now the total emission in SE (Figure 9b′) is compared with the phosphorescence in EtOEt (Figure 8a″) and in SE (Figure 9p′), one can see that the very low value of $\Phi_{P(RH)}$ is due to the inefficiency of the RH $S_1 \rightsquigarrow T$ crossing, caused by an active RH $S_1 \rightarrow S_0$ radiative competition.

Kinetic expression for the chelate formation

With $\Phi_{ST}' \ll \Phi_{ST}$, the expression (33) for the concentration of lowest triplets ^3Y reduces to:

$$[^3Y] = k_3^{*-1}[(^1k_{12}[H^+] + {}^1k)[^1R]\Phi_{ST} - \Phi_{ST} {}^1k_{21}[^1RH] - {}^3k[^3R] - {}^3k'[^3RH]], \quad (34)$$

and from (26) and (34):

$$k_3^*[^3Y] = \Phi_{ST} I_a - {}^3k[^3R] - {}^3k'[^3RH]. \quad (35)$$

Also,

$$\frac{d[Y]}{dt} = k_3^*[^3Y] + k_{23}[RH][BS_4^-] - (k_{32}' + k_{34})[Y] + k_{43}'[X]$$

where $k_{43}' = k_{43}[SH]$ and $k_{32}' = k_{32}[SH]$,

and:

$$(k_{32}' + k_{34})[Y] = \Phi_{ST} I_a + k_{23}[RH][BS_4^-] + k_{43}'[X] - {}^3k[^3R] - {}^3k'[^3RH] \quad (36)$$

Now, for steps (a) and (b) (see Figure 7):

$$\frac{d[R_c]}{dt} = k_1[R] + k_{21}[RH] - (k_{-1} + k_{12}[H^+])[R_c], \quad (37)$$

$$\frac{d[RH]}{dt} = k_{12}[R_c][H^+] + k_2^*[RH^*] + k_{32}'[Y] - (k_{21} + k_{23}[BS_4^-])[RH] - I_a \quad (38)$$

and from (14) to (19) and (30):

$$I_a = ({}^1k' + {}^1k_{21} - {}^1k_{12}[H^+][^1R][^1RH]^{-1})[^1RH] \quad (39)$$

Moreover, with:

$$\varphi'' = {}^1k_{12}[H^+][^1R]/_a, \quad (40)$$

$$\Phi'' = k_2^*[RH^*]/I_a, \quad (41)$$

where

$$k_2^* = {}^1k' \simeq k_F' + k_C' + {}^1k_Q'[Q],$$
$$(k_{ST}' \ll k_F' + k_C' + {}^1k_Q'[Q]),$$
$$[RH^*] = [^1RH],$$

and with (39), (41) becomes:

$$\Phi'' = {}^1k'(1 + \varphi'')/{}^1k' + {}^1k_{21}, \quad (42)$$

giving the following expression for the rate of RH formation:

$$\frac{d[RH]}{dt} = \left(\frac{1 + \varphi''}{1 + {}^1k_{21}{}^1k'^{-1}} - 1\right) I_a + k_{12}[R_c][H^+] + k_{32}'[Y] - (k_{21} + k_{23}BS_4^-)[RH] \quad (43)$$

Assuming steady-state conditions for R_c and RH, and if $k_{-1} \gg k_{12}[H^+]$, the relations (2), (37) and (43) give:

$$[RH] = \frac{k_1 k_{-1}^{-1} {}^1k_{12}[H^+][R] + k_{32}'[Y]}{k_{21} - \varphi^{**}\varepsilon_{RH} V^{-1} G I_o' + k_{23}[BS_4^-]}, \quad (44)$$

where

$$\varphi^{**} = [(1 + \varphi'')/(1 + {}^1k_{21}{}^1k'^{-1})] - 1 \quad (45)$$

Also, considering the fact that most probably $\varphi'' < 1$ and ${}^1k_{21}{}^1k'^{-1} \geq 1$, φ^{**} must have a negative value.

Moreover, assuming that $[BS_4^-]_o \simeq [A]_o$ (see discussion on boron species), and since $[A]_o \gg [R]_o$ (see Experimental), it follows from relations (36) and (44) that:

$$\Phi_{ST} I_o' \varepsilon_R V^{-1} G[R] + \frac{k_1 k_{-1}^{-1} k_{12}[H^+][R]}{\frac{k_{21}}{k_{23}[A]_o} + \frac{\varphi^{**} \varepsilon_{RH} V^{-1} G I_o'}{k_{23}[A]_o} + 1}$$

$$+ k_{43}'[X] - {}^3k[{}^3R] - {}^3k'[{}^3RH] =$$

$$\left(1 - \frac{1}{k_{21} + \varphi^{**} \varepsilon_{RH} V^{-1} G I_o' + k_{23}[A]_o} + \frac{k_{34}}{k_{32}'}\right) k_{32}'[Y] \quad (46)$$

From values of I_o' ($\sim 10^{-5}$), G ($\simeq 1.9$), V ($= 3 \times 10^{-3}$), ε_{RH} (~ 15200), $[A]_o$ ($\sim 10^{-3}$), the term containing φ^{**} in the first member of equation (46) is much larger than unity, while in the second member the fraction containing φ^{**} is negligible, so that (46) reduces to:

$$[Y] = \frac{\Phi_{ST} I_o' \varepsilon_R V^{-1} G[R]}{k_{32}' + k_{34}} + \frac{k_{23} k_1 k_{-1}^{-1} k_{12}[H^+][R][A]_o}{(k_{21} + \varphi^{**} \varepsilon_{RH} V^{-1} G I_o')(k_{32}' + k_{34})} + \frac{k_{43}'[X]}{k_{32}' + k_{34}} + \frac{{}^3k[{}^3R] + {}^3k'[{}^3RH]}{k_{32}' + k_{34}}, \quad (47)$$

leading to the following rate expression for the chelate formation:

$$\frac{d[X]}{dt} = (M + N[A]_o)([R]_o - X) - W[X] - U, \quad (48)$$

where:

$$M = k_{34} \Phi_{ST} I_o' \varepsilon_R V^{-1} G / (k_{32}' + k_{34}) \quad (49)$$

$$N = \frac{k_{34} k_{23} k_1 k_{-1}^{-1} k_{12}[H^+]}{(k_{32}' + k_{34})(k_{21} + \varphi^{**} \varepsilon_{RH} V^{-1} G I_o')} \quad (50)$$

$$W = k_{32}' k_{43}' / (k_{32}' + k_{34}) \quad (51)$$

$$U = ({}^3k[{}^3R] + {}^3k'[{}^3RH]) / (k_{32}' + k_{34}) \quad (52)$$

It is to note that, for a given I_o', M, N and U are constants, so that the solution of (48) is:

$$\ln \frac{[X]_e}{[X]_e - [X]} = k_{ir}^{obs} \cdot t = (\vec{k}_{ir}[A]_o + \overleftarrow{k}_{ir}) t, \quad (53)$$

where:

$$\overleftarrow{k}_{ir} = M \cdot W = (k_{34} \Phi_{ST} I_o' \varepsilon_R V^{-1} G + k_{32}' k_{43}') / (k_{32}' + k_{34}), \quad (54)$$

$$\vec{k}_{ir} = N = \frac{k_{34} k_{23} k_1 k_{-1}^{-1} k_{12}]H^+]}{(k_{32}' + k_{34})(k_{21} + \varphi^{**} \varepsilon_{RH} V^{-1} G I_o')}, \quad (55)$$

$$k_{ir}^{obs} = (M + N[A]_o)[R]_o - U[X]_e^{-1}. \quad (56)$$

As can be seen from (54) and (55), $\overleftarrow{k}_{ir}$ and $\vec{k}_{ir}^{-1}$ are linear functions of I_o', with the reciprocal of the overall forward rate constant $(k_{32}' + k_{34}/k_{34} k_{23} k_1 k_{-1}^{-1} k_{12}[H^+])$ and with the overall reverse rate constant $(k_{32}' k_{43}'/(k_{32}' + k_{34}))$ for dark complexation, as intersections at the origin.

Figure 3 shows that expressions (54) and (55) are in accordance with the experimental results.

Ligand lowest triplet contribution to chelate formation

The validity of relation (54) gives only an indirect kinetic evidence for excited-state ligand contribution to chelate formation.

However, a more direct evidence can be brought from the analysis of expression (56), which contains kinetic terms for triplet degradation processes of the ligand.

In fluid and non-deaerated media (our experimental conditions), steps ${}^3k$, ${}^3R$ and ${}^3k'$, ${}^3RH$ must be important, essentially because of the quenching terms ${}^3k_Q[Q]$ and ${}^3k_Q'[Q]$ (see (27) and (31)).

From the expression (57) (see (56), (55), (42)):

$$k_{ir}^{obs}[X]_e I_o'^{-1} = k_{34} \Phi_{ST} \varepsilon_R V^{-1} G[R]_o / (k_{32}' + k_{34}) - \vec{k}_{ir}[R]_o [A]_o I_o'^{-1} - ({}^3k[{}^3R] + {}^3k'[{}^3RH]) / (k_{32}' + k_{34}) I_o', \quad (57)$$

one would, therefore, expect, for a given $[R]_o$ and $[A]_o$, a non-linear variation:

$$k_{ir}^{obs}[X]_e I_o'^{-1} = f(\vec{k}_{ir}[R]_o [A]_o I_o'^{-1}), \quad (58)$$

with $k_{ir}^{obs}[X]_e I_o'^{-1}$ increasing monotonously with I_o'.

If, however, ligand lowest triplet reversible interaction with boron species takes place and gives the non-chelate intermediate ${}^3Y$ (see (20)), step ${}^3k'$, ${}^3RH$ and consequently ${}^3k$, ${}^3R$ must be more and more quenched as $[A]_o$ increases, linearising progressively (58).

Figure 10 reflects indeed this kinetic behaviour so that, in conclusion, we can propose the following scheme as a mechanism consistent with the experimental results:

$$R \xrightarrow{h\nu} R$$

$${}^1R \rightsquigarrow R$$

$${}^1R \rightsquigarrow {}^3R \rightsquigarrow R$$

$${}^1R \overset{H^+}{\rightleftharpoons} {}^1RH$$

$${}^3R \overset{H^+}{\rightleftharpoons} {}^3RH \rightsquigarrow RH$$

$${}^3RH \overset{BS_4^-}{\rightleftharpoons} {}^3(\overset{+}{R}O\overset{-}{B}S_3) + SH$$

$${}^3(\overset{+}{R}O\overset{-}{B}S_3) \rightsquigarrow \overset{+}{R}O\overset{-}{B}S_3$$

$$R \rightleftharpoons R_c$$

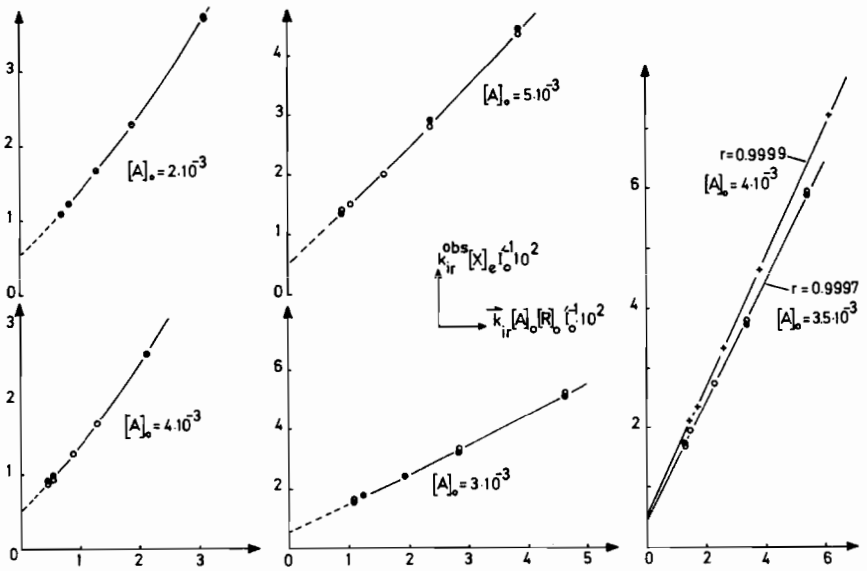

Figure 10. $k_{ir}^{obs}[X]_e I_o'^{-1}$ *vs.* $k_{ir}[R]_o[A]_o I_o'^{-1}$ for various initial boron acid concentrations $[A]_o$ ($[R]_o = 10^{-5} M$). ●- experimental, o- and x- calculated.

$$R_c \overset{H^+}{\rightleftharpoons} RH \qquad {}^1RH \rightsquigarrow RH$$

$$RH \overset{BS_4^-}{\rightleftharpoons} \overset{+}{R}O\bar{B}S_3 + SH \qquad {}^1RH \rightleftharpoons {}^1R + H^+$$

$$\overset{+}{R}O\bar{B}S_3 \rightleftharpoons \overset{+}{R}O_2\bar{B}S_2 + SH \qquad {}^1RH \rightsquigarrow {}^3RH$$

$$RH \xrightarrow{h\nu} {}^1RH$$

Acknowledgements

I am very grateful to Mrs. Y. Zakaria, who carried out most of the experimental work.

References

1 V. Balzani and V. Carassiti, "Photochemistry of Coordination Compounds", Academic Press, London (1970). (a) p. 156.
2 D. Bryce-Smith, "Photochemistry", The Chemical Society, Burlington House, London. *Vol. 1,* p. 119 (1970); *Vol. 2,* p. 235 (1971); *Vol. 3,* p. 293 (1972); *Vol. 4,* p. 355 (1973); *Vol. 5,* p. 261 (1974).
3 A.W. Adamson, *J. Inorg. Nucl. Chem., 13,* 275 (1960).
4 J. Kuo, *Dissertation,* Louisiana State University (1966).
5 S. Nagakura and J. Tanaka, *J. Chem. Phys., 22,* 236 (1954).
5a) This effect has been already explained in terms of the ICT model for substituted acetophenones, 24, 311 (1956).
6 R.J. Gillespie and S. Wasif, *J. Chem. Soc.,* 204 (1953).
7 R.J. Gillespie, J.V. Oubridge and C. Solomons, *J. Chem. Soc.,* 1804 (1957).
8 D. Jaques and J.A. Leisten, *J. Chem. Soc.,* 4963 (1961).
9 M. Marcantonatos, A. Marcantonatos and D. Monnier, *Helv. Chim. Acta, 48,* 194 (1965).
10 S.L. Murov, "Handbook of Photochemistry", M. Dekker, New York (1973), p. 119.
11 M. Marcantonatos and G. Gamba. Results to be published.
12 T.C. Waddington, "Non-aqueous Solvent Systems", Academic Press, London (1965), p. 189.
13 M. Marcantonatos and C. Menzinger, *Inorg. Chim. Acta* (in press).
14 M. Marcantonatos and G. Gamba, *Helv. Chim. Acta, 52,* 2183 (1969).